

Technical note

Undersampling to acquire nuclear magnetic resonance images

Pablo Pérez^a, Andrés Santos^{b,*}

^a Instituto de Ingeniería, UNAM, Mexico

^b Depto. Ingeniería Electrónica, E.T.S.I. Telecomunicación, Universidad Politécnica de Madrid, E-28040 Madrid, Spain

Received 5 August 2003; received in revised form 29 December 2003; accepted 30 January 2004

Abstract

In this paper, we present a method that permits the application of a direct digital receiver based on undersampling techniques to NMR and MRI scanners working with incoherent excitation pulses, and we evaluate the performance of such receivers in the acquisition and reconstruction of images. The method has been tested on a BRUKER BIOSPEC BMT 47/40, and the results show that undersampling can be used to process NMR and MRI signals, and that it correctly reconstructs images without loss of information, extending the range of applications of ‘digital radio’ techniques to NMR and MRI systems working with high-intensity magnetic fields. We also describe a series of tests performed to validate the application of undersampling to NMR systems and an algorithm to compensate the phase fluctuations due to the incoherent excitation pulses.

© 2004 IPPEM. Published by Elsevier Ltd. All rights reserved.

Keywords: Undersampling; Direct digital receiver; NMR and MRI systems; Foldback noise; Image reconstruction

1. Introduction

Several studies have shown that a direct digital receiver based on oversampling or undersampling can replace advantageously the analog sections in traditional MRI systems [1–3]. The use of oversampling is convenient in direct digital receivers for low-field MRI or Overhauser Imaging [3]. However, the application of this technique to high-field NMR and MRI systems is limited by the required sampling frequency of the analog-to-digital converter (ADC) [1]. Such high sampling rates can only be achieved with high-end (and consequently expensive) ADCs with a reduced number of bits of resolution (eight bits in some flash ADCs) and its corresponding low signal-to-noise ratio (SNR). A second disadvantage of these high-rate conversion systems is that they require the use of very fast digital electronics and large storage capacities, or the use of specialized circuits such as digital down converters [4], which do not permit easy adjustment or compensation

for the phase fluctuations in the carrier of the excitation pulses.

As an alternative, the use of undersampling for handling NMR signals has been proposed by Pérez et al. [5], Green and Balcom [6] and Stortmont et al. [7], and has been successfully applied in electron paramagnetic resonance detection [8], and in radio communications, in what has been called ‘software radio’ [9]. In these papers, it has been shown that undersampling can be used to move a bandpass signal at a high-frequency to a lower frequency without loss of information if the process of sampling satisfies the bandpass sampling theorem [10,11]. Undersampling directly applied to the amplified NMR or MRI signal, as shown in Fig. 1, noticeably reduces the speed and storage requirements of the data acquisition system, and therefore the cost of equipment. Undersampling permits extension of the application of digital techniques to a larger set of NMR systems, including low, medium and high magnetic field systems. However, it is necessary to take into account the fact that the direct digital receiver structure shown in Fig. 1, which is convenient for an MRI system working with coherent excitation pulses, needs to be adapted for systems working with

* Corresponding author. Tel.: +34-91-336-6827; fax: +34-91-336-7323.

E-mail address: andres@die.upm.es (A. Santos).

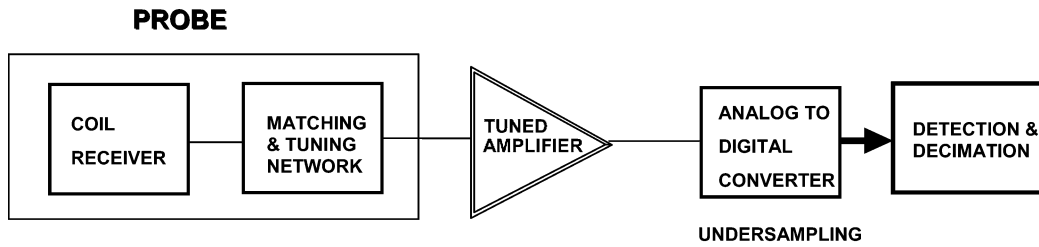


Fig. 1. Block diagram of the direct digital receiver proposed for an NMR system working with coherent excitation pulses. After the tuned amplifier, the signal is down-converted with undersampling. The last block (detection and decimation) is used if the demodulated signal is not centered at zero frequency.

incoherent excitation pulses, as shown below. This type of pulse is used in many commercial systems.

This work presents the use of the undersampling or passband sampling technique in the acquisition of NMR signals for image reconstruction applied to commercial analog equipment working with incoherent excitation pulses. A method of compensation for phase fluctuations between lines of the k -space, due to the incoherent excitation pulses, is also presented. This method permits correct reconstruction of the images and shows that the use of undersampling does not introduce any loss of information. Section 2 briefly introduces the theoretical basis of undersampling, Section 3 presents the experiments performed to confirm the predictions, and the results are shown and discussed in Section 4. Finally, conclusions are presented in Section 5.

2. Theory

Bandpass signals are characterized by having no frequency components above a frequency f_h or below a frequency f_l . As shown in various references (for example [10,11]) the aliasing produced during the sampling process can be used advantageously when sampling passband signals: a sampling rate lower than $2f_h$ can be used, according to the bandpass sampling theorem for uniform and instantaneous sampling. This theorem states that a bandpass signal can be reproduced from its sample values if the sampling frequency f_s satisfies [10]

$$\frac{2f_h}{n} \leq f_s \leq \frac{2f_l}{(n-1)} \quad (1)$$

where n is an integer that satisfies

$$2 \leq n \leq \frac{f_h}{(f_h - f_l)} \quad (2)$$

and

$$[f_h - f_l] \leq f_l \quad (3)$$

As has been illustrated in previous work [5,10], sampling a bandpass signal with a sampling frequency that

satisfies the constraints established in Eq. (1) produces a sequence of samples that permits recovery of the original analog signal spectrum centered at a lower frequency. In general, this latter frequency is not zero, except in certain conditions [12]. An additional constraint is that the sampled signal must have a sampling frequency greater than twice its bandwidth. Therefore, it is necessary to perform a numerical demodulation to move the signal to the baseband and realize a decimation process to reduce the sampling frequency to that required by the Nyquist theorem. These processes are depicted in Fig. 1 as detection and decimation.

Other characteristics of the ADCs that become important when they are used beyond the Nyquist rate or with undersampling have been studied in the literature [11]; one of the most relevant is the degradation of the SNR. In general, the thermal noise and the quantization error spectra present extend well beyond the Nyquist frequency f_s ($f_s = 2B$, B being the signal bandwidth). When a quantized signal is sampled, the entire noise spectrum is folded back into the baseband (aliasing), and it is reasonable to take the total quantization noise power as a measure of the noise to be expected in the baseband [13,14]. For sinusoidal inputs, an expression for the maximum theoretical signal-to-quantization-noise ratio at the Nyquist rate can be derived following certain assumptions on the noise and the input signal [15,16]:

$$\text{SNR} = 6.02N + 1.76 \text{ dB} \quad (4)$$

where N is the number of bits of the ADC. As is well known, for each extra bit of resolution in the ADC, there is approximately 6 dB improvement in the SNR.

In the case of undersampling applied to relocate a bandpass signal, the noise from all the aliased bands is combined into the band where the signal of interest is relocated. As in any sampled system, the periodicity of the spectrum causes all wideband noise to be combined in each of the $f_s/2$ bands. Even with an ideal antialiasing filter, the SNR is not preserved in bandpass sampling because the noise from the aliased spectra will always overlap into the signal.

An estimation of the degradation of the SNR ratio can be obtained, considering that the noise spectrum is not uniform, according to the following formula [13]:

$$D_{\text{SNR}} \approx 10 \log \left(\frac{B_{\text{EA}}}{f_s/2} \right) \quad (5)$$

where f_s is the sampling rate and B_{EA} is the equivalent noise bandwidth of the analog signal. This degradation behavior has been shown experimentally [13] and in the field of NMR [5]. As shown in Eq. (5), the degradation of the SNR can be reduced if the equivalent noise bandwidth of the analog signal is reduced using a better passband filtering process in the radio-frequency (RF) stage (before the signal is applied to the input of the ADC) and increasing the number of bits of resolution of the ADC (smaller quantization noise). When the noise level obtained with a certain sampling frequency is unacceptable, it can be reduced by using a higher sampling frequency.

As presented above, undersampling degrades the SNR, but because an analog phase-quadrature detector (the standard circuit used in NMR and MRI systems) also introduces some degradation, there may be an overall improvement in SNR. As an example and according to the literature until 1997 [17–19], the degradation produced by phase-quadrature detectors was at least 10 dB (nowadays quadrature phase detectors with insert loss of about 1 dB can be found [20]). Therefore, from Eq. (5), it can be deduced that by choosing an adequate sampling frequency, undersampling could provide a SNR similar to that obtained with an analog phase-quadrature detector. Nevertheless, this comparison is between the two components working isolated and with an input signal with the same characteristics. In a NMR system, these components are part of a signal processing chain in which the noise figure of the pre-amplifier will predominate [21,22]. Digital undersampling with substantial degree of undersampling, can be advantageous in terms of SNR, when replacing noisy quadrature receivers.

Note that when applying digital techniques in parallel to the original analog system to acquire the NMR RF signal, as in this work, the coherence of the excitation pulses applied to the sample during excitation is important. The oscillating RF field produced by the transmitter coil when a sequence of pulses is applied at times t_1, t_2, \dots, t_k with duration $\tau_1, \tau_2, \dots, \tau_k$ can be represented by the following function [23]

$$H(t) = \sum_k A_k(t) \cos(\omega t + \varphi_k) \quad (6)$$

where $A_k(t) = 0$ outside the interval $t_k \leq t \leq t_k + \tau_k$. These pulses are called incoherent if the phases φ_k are randomly distributed, and coherent if their values can be controlled (in particular, if they have the same value φ). These variations in phase values clearly affect the

final phase of the received signal, especially the encoding phase in a 2DFT image reconstruction process. If coherent pulses are used, the receiver structure presented in Fig. 1 is still valid, because in this case, the phase of the received signal is not modified from line to line in the scanning process. However, when the NMR equipment uses incoherent pulses, it is necessary either to have a reference signal or to implement a method to compensate for the phase fluctuations. If these phase fluctuations are uncompensated, a reconstructed image similar to that shown in Fig. 2 is obtained. Then, to reconstruct the image, it is necessary to acquire either the reference signal used by the analog demodulation stage in the NMR equipment, or the excitation pulse itself to estimate the initial phase. Then, the system structure in Fig. 1 has to be modified to include additional stages to acquire the excitation pulses and the echoes as shown in Fig. 3.

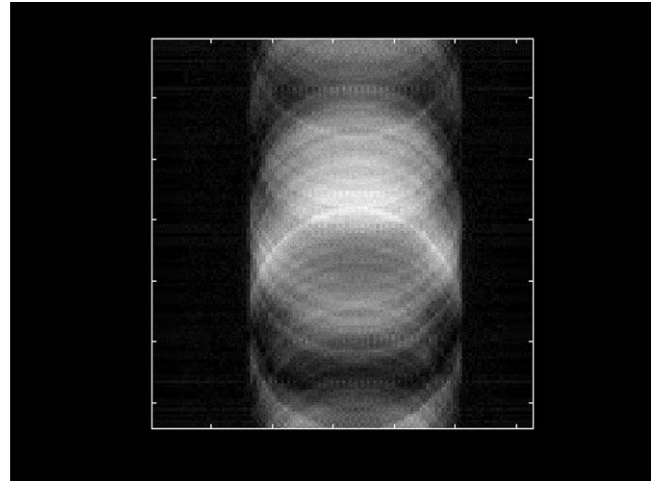


Fig. 2. A cross-section image reconstructed without compensation for the received signal phase fluctuations.

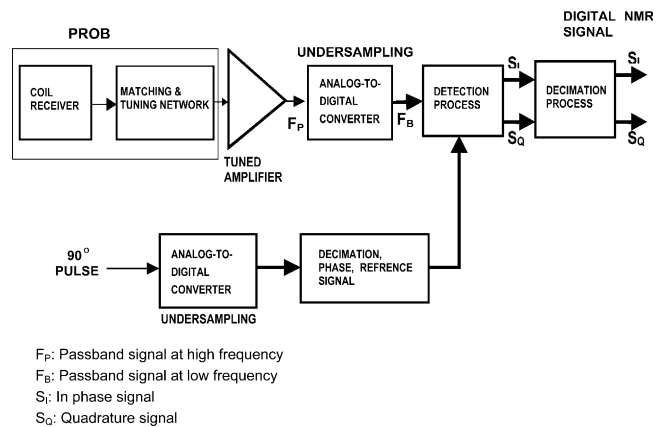


Fig. 3. Direct digital receiver proposed for an NMR system working with incoherent excitation pulses when the reference signal used in the analog quadrature detection is not available.

3. Materials and methods

The proposed method for acquiring MR images with undersampling, including the compensation for phase fluctuations due to the incoherence of the excitation pulses, was tested on a BIOSPEC BMT 47/40 MR system (BRUKER, 4.7 T, 200 MHz for ^1H), which is an analog system up to where the baseband signal is obtained and digitized. It operates using incoherent 90° and 180° excitation pulses.

In our experiments, digital signals were acquired with an oscilloscope (Tektronix TDS-524A with GPIB interface) that has an analog bandwidth limited to 500 MHz per channel, sampling rates up to 500 Msamples/s, and storage capacity up to 50,000 samples per channel. Data were transferred to a personal computer via the GPIB interface after acquisition. One of this oscilloscope's limitations is that it has a resolution of eight bits per sample, which limits the maximum theoretical SNR for every scale to 49.92 dB (Eq. (4)).

The NMR signal (passband, center frequency of 200.36 MHz) was acquired at the input of the BIOSPEC scanner's phase-quadrature detector, where the amplitude of the signal is limited to 100 mV to avoid saturation of the detector, and the bandwidth is 50 kHz or less, depending on the conditions of operation (mainly sequence and FOV). For comparison purposes, the signal at the output of the analog receiver was also acquired immediately before the AD converters and after the analog amplification and filtering processes. At this second point, the echo signal is in quadrature. The connections used are shown in Fig. 4.

Two different phantoms were used in the developed experiments: the first was a 49.5 mm diameter spherical phantom made of glass and filled with water, with a bubble, and the second was a quality control multi-purpose phantom with a complex structure and filled with a H_2O solution which has a $T_1 = 200$ ms. This phantom is supplied by the system manufacturer (BRUKER). In the experiments, the echo signals were

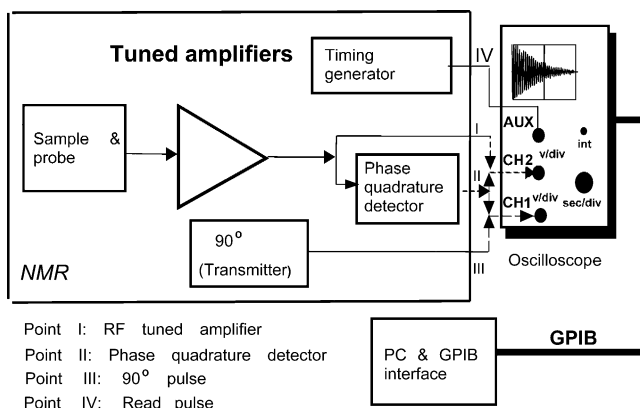


Fig. 4. Interconnection of the equipment used in the experiments.

generated using a spin-echo sequence with $\text{TR} = 1500$ ms and $\text{TE} = 6$ ms. For the spherical phantom, other important data were $\text{FOV} = 60 \times 60 \text{ mm}^2$ and slice thickness = 5 mm, and for the quality control phantom these were $\text{FOV} = 70 \times 70 \text{ mm}^2$ and slice thickness = 4 mm. The acquired data were sent to the computer via the GPIB interface during the TR interval, for processing off-line.

The images of the transverse section of the phantoms were acquired with a resolution of 128×128 pixels. The k-space signals were acquired at the RF output using an undersampling rate of 5 Msamples/s. In all cases, each signal was acquired during an interval of 2.3 ms and its acquisition started with the leading edge of the read pulse. The values of the parameter set for the operation of the NMR system and the oscilloscope permitted us to fulfill the conditions established by the passband sampling theorem, as per Eqs. (1)–(3).

In all cases, it was necessary to develop a method to compensate for the phase fluctuations due to the incoherence of the 90° excitation pulses. As it was not possible to access the reference signal used in the quadrature detection by the BRUKER equipment, it was necessary to acquire the 90° excitation pulses directly using a second oscilloscope channel. For this reason, the oscilloscope was programmed with a pre-event time of 7.7 ms. These excitation pulses allowed us to implement the phase compensation algorithm, and they were acquired and sent to the PC together with the corresponding echo for each of the k-space line. The reconstructed images were compared with those reconstructed with the data acquired after the quadrature receiver at 2.5 Msamples/s (for the spherical phantom) and with the image supplied by the scanner under normal conditions (for the quality phantom) to determine whether the information coded in phase and frequency had been correctly recovered.

The undersampled signals were processed as follows:

- (1) *Carrier frequency detection*, by locating the position of the maximum in the magnitude spectrum of the FID signal, was obtained during the calibration process of the BRUKER system.
- (2) *Baseband shifting*, by multiplying each signal by a complex exponential $\exp(2\pi f_c n / f_s + \varphi_i)$, where f_c is the carrier frequency of the signal, f_s is the sampling rate and φ_i is the phase value that permits compensation for the phase fluctuation of the carrier of the excitation pulses. This phase was obtained using the method outlined in the flow diagram in Fig. 5 and described next [24]. The chosen value of the phase φ is that which produces a positive amplitude, v_{pi} greater than the absolute value of the negative amplitude, $|v_{ni}|$, of the in-phase component from the 90° excitation pulse. It also has the minimum area under the quadrature

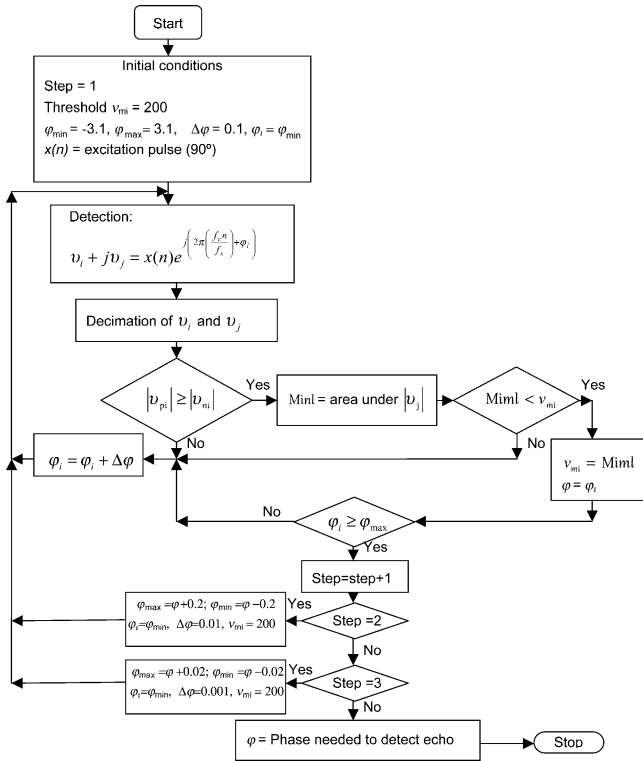


Fig. 5. Flow diagram of the algorithm used to select the adequate phase for detecting the echo signal. This phase produces an envelope with maximum positive real part and minimum imaginary part.

component. This value is computed using a search procedure, which starts with a value $\phi_i = -3.1$ and runs over the interval $-3.1 \leq \phi_i \leq 3.1$, increasing in steps of 0.1. At each step and after multiplying the pulse by the complex exponential and decimating, if the first condition holds, then the area under the quadrature component is computed and compared with the value of the previous step. If the new value is smaller than the previous value, then this new value replaces the previous value, and, at the same time, its corresponding phase value is selected as a better approximation to the final phase, ϕ . If the new value is greater than the previous value, then the old value is retained. A better value of the phase is obtained by repeating the procedure over the interval $[\phi - 0.2, \phi + 0.2]$, using a step size of 0.01. Finally, the procedure is repeated in the interval $[\phi - 0.02, \phi + 0.02]$, with a step size of 0.001. Later, the phase of each of the acquired echoes is corrected using this phase, ϕ , obtained from the 90° pulse. As can be seen, this process tries to obtain a maximum real component and a minimum imaginary component of the 90° pulses. It is important to note that we could have established other conditions for the real and imaginary components, provided that these conditions were retained for the entire process.

- (3) *Decimation*: 128 complex values of each signal, including its quadrature components, were kept to match the scanner data size. These values were stored in a 128×128 matrix, which corresponds to the k-space.
- (4) *Computation of magnitude and phase images*: by applying a complex two-dimensional Fast Fourier Transform (FFT), two 128×128 matrices (magnitude and phase) were computed and stored. In the case of the quality control phantom, only the magnitude matrix was computed.
- (5) *Calculation of SNR*: an estimation of the SNR in the magnitude image was made using the following equation [25]:

$$\text{SNR} = 20 \log \left(\frac{S}{\sigma} \right), \quad \sigma = \frac{\sigma_r}{0.655},$$

$$S = \sqrt{\bar{s}^2 + \sigma_s^2 - 2\sigma^2} \quad (7)$$

where \bar{s} and σ_s are the signal mean values and the signal standard deviation in a 20×20 -pixel region of highest homogeneity, respectively, and σ_r is the noise standard deviation in a 20×20 -pixel background region. It is important to note here, that Eq. (7) is only valid for conventional RF coils, as it is the case here. When using phased arrays, different noise statistics should be considered [26,27].

The signals acquired after the analog mixer (oversampled) were processed using only the last three steps.

4. Results and discussion

If the phase relationship between the lines of the k-space is preserved, then it is possible to reconstruct images, as shown in Figs. 6–8. The reconstructed images show similar structures and dimensions; however, in the examples shown, the image obtained from the undersampled data contains more background noise.

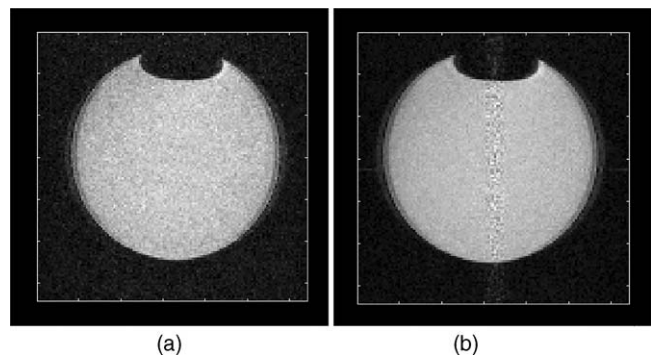


Fig. 6. Reconstructed magnitude images of a sphere filled with water and a bubble. (a) Data acquired after RF stages using undersampling (5 Msamples/s). (b) Data acquired after quadrature receiver using oversampling (2.5 Msamples/s).

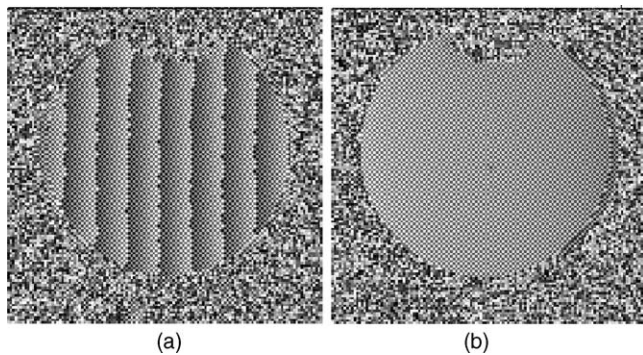


Fig. 7. Reconstructed phase images of a sphere filled with water and a bubble. (a) Data acquired after RF stages using undersampling (5 Msamples/s). (b) Data acquired after quadrature receiver using oversampling (2.5 Msamples/s).

Evaluating the images shown in Fig. 6 using Eq. (7), an SNR of 22.6 dB is obtained for the undersampled acquisition (Fig. 6(a)) and an SNR of 28.1 dB for the oversampled acquisition (Fig. 6(b)). Although, apparently, these data do not encourage the use of undersampling, it should be noted that this is a difficult case—sampling a signal of more than 200 MHz at only 5 Msamples/s. In any case, this difference in SNR between the images is in full agreement with Eq. (5). Obviously, a better SNR can be obtained by using a higher sampling rate.

The artifact in the center of the image in Fig. 6(b) is due to low-frequency noise (approximately 1.2 kHz) in the analog receiver section that processes the imaginary part (a malfunction of the equipment at the time of the experiments). This artifact does not appear in the image reconstructed from the undersampled data, because data were acquired from the signal before the analog receiver section. This confirms that we avoid the problems due to the many sources of noise that may appear during the analog quadrature detection when a direct digital receiver is not used to handle the NMR signals.

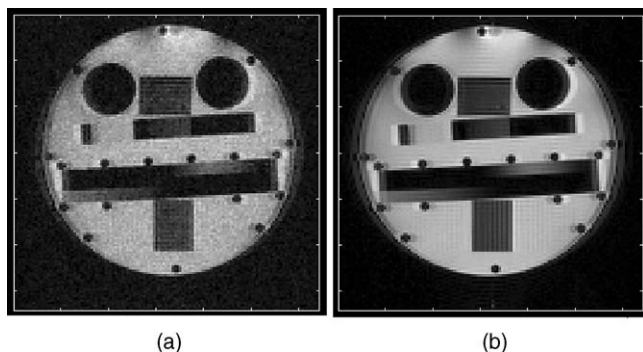


Fig. 8. Images of quality control phantom obtained (a) using undersampling at 5 Ms/s, translation to zero center frequency and compensation of phase and decimation and (b) using the standard BRUKER equipment.

Although Fig. 6(a) shows that the method for recovery of the phase information is correct—at least for objects with a very simple structure—Fig. 7(a), the reconstructed phase image, gives a better demonstration by showing that the phase relation between the lines is correct. The difference between the images in Fig. 7(a) and (b)—specifically, the bands inside the circle in Fig. 7(a)—is due to the different procedures for handling the signals, which give different initial phases. As the phases of the reference signals used in the detection process in both cases (direct digital receiver based on undersampling and analog quadrature detector) are different, the position of the magnetization in the rotating plane, as viewed by the two systems, has different orientation.

Using the 128 signals acquired from the quality control phantom, its modulus image was reconstructed. This image and the corresponding image obtained by the BRUKER equipment are presented in Fig. 8(a) and (b), respectively. There is good correspondence between these two images, but that obtained using undersampling contains more noise. This noise is due to the low resolution of the oscilloscope's ADC, and the very low sampling rate. This example shows that even in the case of objects with a very complex structure, a direct digital receiver based on undersampling allows us to recover the images, if the correct method is used to compensate for the phase fluctuations introduced by the phase fluctuations in the carrier of the 90° pulses.

5. Conclusions

This work presents undersampling as an alternative means of processing NMR and MRI signals to reconstruct the magnitude and phase images. Even in difficult conditions, such as those shown here (very low sampling rate, low number of bits), the images are correctly recovered. Our experimental results have allowed us to confirm that the SNR decreases owing to the folding back of the aliased spectra. However, the method has other advantages, as it eliminates some analog electronic circuits, replacing them with digital processing; it is then possible to ensure that real and imaginary parts are quite symmetric, and that periodic adjustment of the quadrature channels is not required. In addition, as can be seen in the images, this technique overcomes some of the problems that may appear when using analog circuits in radio-frequency processing—for example, low-frequency noise generated by various noise sources and dc offsets. On the other hand, with undersampling, the speed and storage requirements are considerably reduced in comparison with digital systems working with the Nyquist criteria and oversampling. Finally, it has been shown that the information coded in frequency and phase is correctly

recovered after using undersampling; and that in an NMR system working with incoherent excitation pulses, a compensation method, similar to that proposed here, can recover the phase information.

Acknowledgements

The authors thank the Magnetic Resonance Unit of the Instituto Pluridisciplinar (UCM) for allowing us to use their BRUKER equipment, especially Dr. Jesús Ruiz-Cabello, Palmira Villa and Marien Fernández for their help with the setup of our experiments. P. Pérez also thanks CONACYT that has supported part of his work (Project I39157-A). A. Santos acknowledges partial support from TIC2001-0175-C03 (Ministerio de Ciencia y Tecnología) and from G03/185 (Ministerio de Sanidad y Consumo).

References

- [1] Halánek J, Kasal M, Vondra V, Villa M, Cofrancesco P. Direct digital receiver for NMR and MRI. *Magn Reson Mat Phys Biol Med (MAG*MA)* 1996;4(Suppl 2):276.
- [2] Pérez P, Santos A, Vaquero JJ, Rivera M, del Pozo F. Reducing analog circuitry by sampling NMR signals at low speeds. *Magn Reson Mat Phys Biol Med (MAG*MA)* 1996;4:100.
- [3] Luyten MJ, Korbee D, Claasen-Vujcic T, Mehlkopf AF. Programmable direct receiver for low field magnetic resonance imaging. *Proceedings of SMR/ESMRMB, Nice, France. 1995, p. 934.*
- [4] Harris Semiconductor. *Digital signal processing databook*. Harris Semiconductor Literature Department; 1994.
- [5] Pérez P, Santos A, Vaquero JJ. Potential use of the undersampling technique in the acquisition of nuclear magnetic resonance signals. *Magn Reson Mat Phys Biol Med (MAG*MA)* 2001;13:109–17.
- [6] Green DP, Balcom BJ. Undersampling the NMR signal. *Experimental Nuclear Magnetic Resonance Conference, Asilomar (CA). 1998.*
- [7] Stormont RS, Anas MC, Pelc NJ. Radio frequency receiver for a NMR instrument. US patent number 4992736, 1989.
- [8] Hyde JS, Mchaourab HS, Camenisch TG, Ratke JJ, Cox RW, Froncisz W. Electron paramagnetic resonance detection by time-locked subsampling. *Rev Sci Instrum* 1998;69:2622–8.
- [9] Analog Devices Inc. Software radios. *Microwave J* 1996;39:128–136.
- [10] Brigham EO. *The fast Fourier transform and its application*. New Jersey: Prentice-Hall; 1988.
- [11] Wepman JA. Analog-to-digital converters and their applications in radio receivers. *IEEE Commun Mag* 1995;33:39–45.
- [12] Varosi SM, Duensing GR, Fitzsimmons JR. Multiplexing applied to a digital MR receiver. *Proceedings of SMR/ESMRMB, Nice, France. 1995, p. 1009.*
- [13] Vaughan RG, Scott NL, White DR. The theory of bandpass sampling. *IEEE Trans Signal Process* 1991;39:1973–84.
- [14] Cattermole KW. *Principles of pulse code modulation*. London: Iliffe Books; 1969.
- [15] Ifeachor EC, Jervis BW. *Digital signal processing. A practical approach*, 1st ed.. New York: Addison-Wesley; 1993.
- [16] Aziz PM, Sorensen HV, Der Spiegel JV. An overview of sigma-delta converters. *IEEE Signal Process Mag* 1996;13:61–84.
- [17] Microwave Communications Laboratories, Inc. Single sideband quadrature modulators/demodulators. Available from: <http://mclci.com/quadratu.html>, 1997.
- [18] Chen C-N, Hoult DI. *Biomedical magnetic resonance technology*. Bristol: Adam Hilger; 1989.
- [19] Rhode UL, Whitaker J, Bucher TTN. *Communications receivers: principles and design*, 2nd ed. New York: McGraw-Hill; 1997.
- [20] Tayloe D. A low-noise, high-performance zero IF quadrature detector/preamplifier. *RF Design*. Available from: http://rfdesign.com/ar/radio_lownoise_highperformance_zero/index.htm, March, 2003.
- [21] Vlaardingerbroek M, den Boer JA. *Magnetic resonance imaging: theory and practice*. Berlin: Springer-Verlag; 1996.
- [22] Redpath TW, Wiggins CJ. Estimating achievable signal-to-noise ratios of MRI transmit-receive coils from radiofrequency power measurements: applications in quality control. *Phys Med Biol* 2000;45:217–27.
- [23] Abragam A. *Principles of nuclear magnetism*. Oxford: Clarendon Press; 1994 [reprint].
- [24] Perez P. *Adquisición de imágenes de resonancia magnética nuclear mediante técnicas de submuestreo*. PhD thesis, Universidad Politécnica de Madrid, Madrid; 1999.
- [25] Henkelman RM. Measurement of signal intensities in the presence of noise in MR images. *Med Phys* 1985;12:232–3.
- [26] Constantinides CD, Atalar E, McVeigh ER. Signal-to-noise measurements in magnitude images from NMR paced arrays. *Mag Res Med* 1997;38:852–7.
- [27] Edelstein WA, Bottomly PA, Pfeifer LM. A signal-to-noise calibration procedure for NMR imaging systems. *Med Phys* 1984;11:180–5.